International Journal of Chemistry Research

Online ISSN- 0976-5689 Vol 8, Issue 4, 2024

Research Article

ANTIMICROBIAL, ANTIOXIDANT AND CYTOTOXICITY STUDY OF Cu(II), Zn(II), Ni(II), AND Zr(IV) COMPLEXES CONTAINING O, N DONOR SCHIFF BASE LIGAND

SAJIB HOSSAIN[1], ASHRAFUL ISLAM[1], FARIA TASNIM[2], FARUK HOSSEN[1], KUDRAT-E-ZAHAN[1], ALI ASRAF[1]*

[1]Department of Chemistry, University of Rajshahi, Rajshahi-6205, Bangladesh. [2]Department of Genetic Engineering and Biotechnology, University of Rajshahi, Rajshahi-6205, Bangladesh

***Corresponding author: Ali Asraf; *Email: asraf.chem@ru.ac.bd**

Received: 10 Jul 2024 Revised and Accepted: 15 Aug 2024

ABSTRACT

Objective: The aim of the research is to synthesize and characterize Cu(II), Zn(II), Ni(II), and Zr(IV) complexes with a Schiff base ligand, and evaluate their antibacterial and antioxidant properties.

Methods: The ligand was synthesized by refluxing salicylaldehyde with *o*-phenylenediamine in ethanol, forming a yellow-orange product. The complexation reaction involved stirring ethanolic solutions of Zn(II), Cu(II), Ni(II), or Zr(IV) salts with a Schiff base ligand. Thermal decomposition of Zn(II), Cu(II), Ni(II), and Zr(IV) complexes was analyzed under nitrogen, heating at 30 °C/min, measuring weight loss from ambient temperature to 800 °C. The antibacterial activity, antioxidant properties, and cytotoxicity of the synthesized compounds wereexamined using reported methods.

Results: Cu(II), Zn(II), Ni(II), and Zr(IV) complexes with a Schiff base ligand were synthesized. Analyzed through Fourier-transform infrared spectroscopy (FTIR), Ultraviolet-visible (UV-vis) and physiochemical tests and confirmed the structures. Magnetic susceptibility and electronic spectra suggested geometries, supported by thermogravimetric data. Antibacterial tests revealed complexes had higher activity than ligands, and also showed antioxidant properties.

Conclusion: Cu(II), Zn(II), Ni(II), and Zr(IV) Schiff base complexes were synthesized, showing tetrahedral or square planar geometries. They exhibited thermal stability and strong antibacterial activity, outperforming the ligand alone.

Keywords: Schiff base, Transition metal complex, Spectral analysis, Electronic spectra thermogravimetric analysis, Antibacterial activity, Antioxidant, Cytotoxicity

DOI: http://dx.doi.org/10.22159/ijcr.2024v8i4.231 Journal homepage: https://ijcr.info/index.php/journal

INTRODUCTION

Hugo Schiff (1864) gave the term "Schiff base ligand" to this compound, which is created when an active carbonyl group condenses with a primary amine-containing azomethine (CH=N) group, replacing the carbonyl group of an aldehyde or ketone under appropriate conditions. Due to its biological and industrial applications, Schiff base metal complexes have been the subject of extensive investigation since 1930 [1-3]. Due to their prospective use in catalysis, medicine, and material science, Schiff bases containing nitrogen and phenolic oxygen donor atoms are of immense importance [4, 5]. These ligands exhibit unpredictable configurations, structural liability, and sensitivity to molecular environments in their transition metal complexes. These complexes' core metal ions serve as pharmacological drug active sites [5, 6]. In addition to their well-known biological effects, Schiff bases and their metal complexes also play an important role in medicine and the pharmaceutical industry and exhibit some degree of antibacterial, antifungal, antitumor, anticancer, and anti-inflammatory activity [7-11]. It is the azomethine connection that gives Schiff bases their biological action. A few N, O donor Schiff bases and associated transition metal complexes have recently been synthesized by our team [12-19]. This report describes the synthesis, characterization and biological activity evaluation of Cu(II), Zn(II), Ni(II), and Zr(IV) complexes containing Schiff base ligand derived from salicylaldehyde and *o-phenylenediamine*. The ever-increasing metal complexes in various fields of science are the driving force for the research and coordination chemistry. Coordination chemistry plays an outstanding role in the biological process that causes interesting changes i. e. change of oxidation number, change. This is in part due to the extensive and important of such complexes in bio-inorganic chemistry. It has now been well established that many of the chemical elements including metal ions control a vast range of biological processes, thus giving a new dimension to coordination chemistry. Coordination chemistry has its greatest application in the field of hydrometallurgy and pyrometallurgical operations [1-3]. Many metal complexes find applications in the field of catalysis. Among the top performers in this class (and the elements involved) is the Wilkinson catalyst for the hydroformylation reaction (Rh), the conversion of ethylene to acetaldehyde (Ph) and olefin polymerization (Zr, Ni); there are many others too numerous to mention. It should also be noted that one of the greatest recent advances in organic chemistry, asymmetric synthesis, which depends entirely upon transitional metal atoms as the catalytic centers [22, 23].

MATERIALS AND METHODS

Chemicals and reagents

We utilized commercially procured chemicals in their original state, without any additional purification. The subsequent compounds are as follows: The following chemicals were obtained from Sigma Aldrich, India: salicylaldehyde, o-phenylenediamine, Zn (II) sulphate heptahydrate, Cu(II) chloride dihydrate, Ni(II) sulphate hexahydrate, Zr(IV) nitrate pentahydrate, DMSO (dimethyl sulfoxide), and 1,1-Diphenyl-1-p. In this investigation, we utilized analytical-grade organic solvents, including ethanol, methanol, and DMF (dimethylformamide), without the need for any additional purification.

Instrumentation

In this investigation, a variety of analytical methodologies were implemented to characterize metal complexes and ligands. The AZ6512 electrothermal melting point device was employed to ascertain the melting points. The FTIR-8400 SHIMADZU infrared spectrophotometer was

employed to record infrared spectra with KBr discs. The UV spectra were acquired using a Shimadzu Double Beam spectrophotometer (UV 1200 and UV-1650PC) at a concentration of 5×10–4 M. The sherwood scientific magnetic susceptibility balance was employed to quantify the magnetic moments of solid complexes.

Experimental

Synthesis of schiff base ligand $C_{20}H_{16}O_2N_2$(L)

Ligand was prepared by the condensation reaction of 20 mmol of salicylaldehyde (2.1 ml) with 10 mmol (1.08g) of o-phenylenediamine in a round-bottomed flask. Salicylaldehyde was dissolved in 20 ml ethanol and *o*-phenylenediamine was dissolved in hot ethanol. The solutions were mixed and refluxed for 4 h. On cooling yellow-orange colored product was formed which was washed with ethanol, acetone, and diethyl ether and dried in vacuum desiccators over anhydrouscalcium chloride($CaCl_2$). The progress and purity of the ligand were tested by Thin layer chromatography (TLC) using different solvents. The product was found to be soluble in methanol, chloroform, and Dimethyl sulfoxide(DMSO). It provided 90% yield, color-yellow orange (fig. 1).

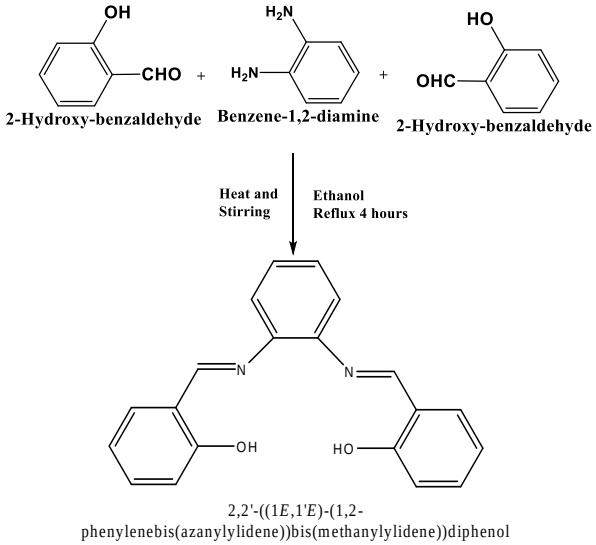

Fig. 1: Synthesis route of Schiff base ligand $C_{20}H_{16}O_2N_2$

Synthesis of Zn(II), Cu(II), Ni(II), Zr(IV) complexes with Schiff base ligand $C_{20}H_{16}O_2N_2$

During complexation reaction,15 ml ethanolic solution of Zn (II) sulphate heptahydrate (0.287g, 1 mmol) or Cu(II) chloride dihydrate (0.170g, 1 mmol)or Ni(II) sulphate hexahydrate (0.262g, 1 mmol)or Zr(IV) nitrate pentahydrate(0.399g, 1 mmol) was taken in a two necked round bottom flask and kept on a magnetic stirring. An ethanolic solution (20 ml) of prepared Schiff base ligand (0.316g, 1 mmol) was added dropwise with constant stirring on a magnetic stirrer for 4-5 h. On cooling, a colored solid product was formed, which was washed with methanol and dried in a vacuum over anhydrous calcium chloride ($CaCl_2$). The reaction was monitored by thin layer chromatography (TLC) using petroleum ether, toluene, ethyl acetate, and methanol as solvent. The complexes were soluble in dimethyl sulfoxide (DMSO). The target Schiff base and proposed structure of metal complexes are shown in (fig. 2)

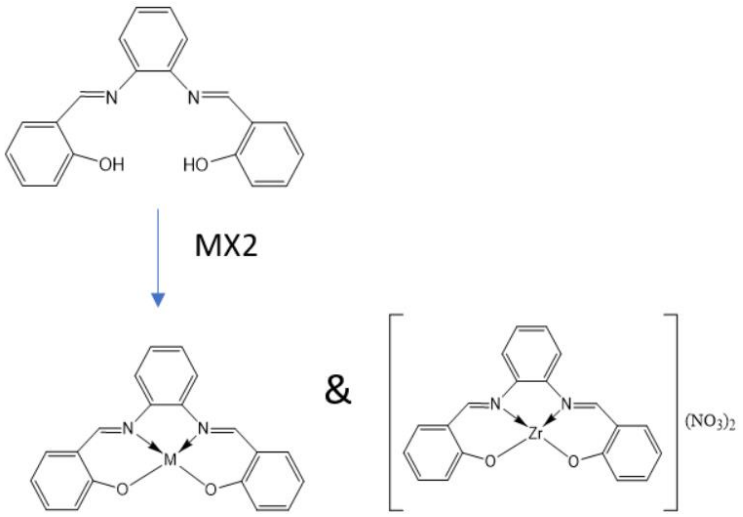

Fig. 2: Synthesis route of metal complexes where, M= Zn(II), Cu(II), Ni(II), and Zr(IV) ion

RESULTS AND DISCUSSION

Physical properties

Some physical properties of the Schiff base ligand and its metal complexes, such as melting point, color, pH, and conductivity, are shown in (table 1). The complexes are intensely colored, powder solids, which decompose above 300 °C. Molar conductance values of the complexes in aqueous solution and dimethyl sulfoxide DMSO (10^{-3}M) showed low values (7-9 µS/cm), indicating them to be non-electrolytes shown in (table 1). The complex of Zr(IV) shows electrolytic behavior in DMSO solution.

Table 1: Physical characteristics and analytical data of ligands and complexes

Compounds/mol. formula	Formula weight (g/mol	Color	Yield (%)	M. P (°C)/(decomp)	Conductivity (µS/cm)
Ligand (L) $C_{20}H_{16}O_2N_2$	316	Yellow	90 %	160	-
[Zn (L)] $[ZnC_{20}H_{14}O_2N_2]$	379.7	Yellow	75%	210	4
[Cu (L)] $[CuC_{20}H_{14}O_2N_2]$	377.5	Green	70%	245	3
[Ni(L)] $[NiC_{20}H_{14}O_2N_2]$	372.7	Red	75 %	>300	2
[Zr(L)] $[ZrC_{20}H_{14}O_2N_2]$ $(NO_3)_2$	529.2	Lemon yellow	75%	> 300	126

Infrared spectroscopy

FT-IR spectra of the Schiff base and its metal complexes are shown in fig. 3 prominent band observed between 1610 cm^{-1} and 1640 cm^{-1} is indicative of the azomethine (HC=N) group [17-19]. The presence of weak broadband in the ligands' IR spectra between (3550 and 3200 cm^{-1}) may be because of the phenolic (-OH) group. When the ligand coordinated with metal ions on complexation, the band for azomethine shifted to a lower frequency, confirming the coordination of the azomethine group [18, 19]. The appearance of new bands at (502-575) cm^{-1} and (350-470) cm^{-1} in the spectra of metal complexes attributed to the metal-oxygen (M-O) and metal-nitrogen (M-N) bond stretching, respectively, and indicating the coordination via phenolic oxygen and azomethine nitrogen atoms [19, 20].

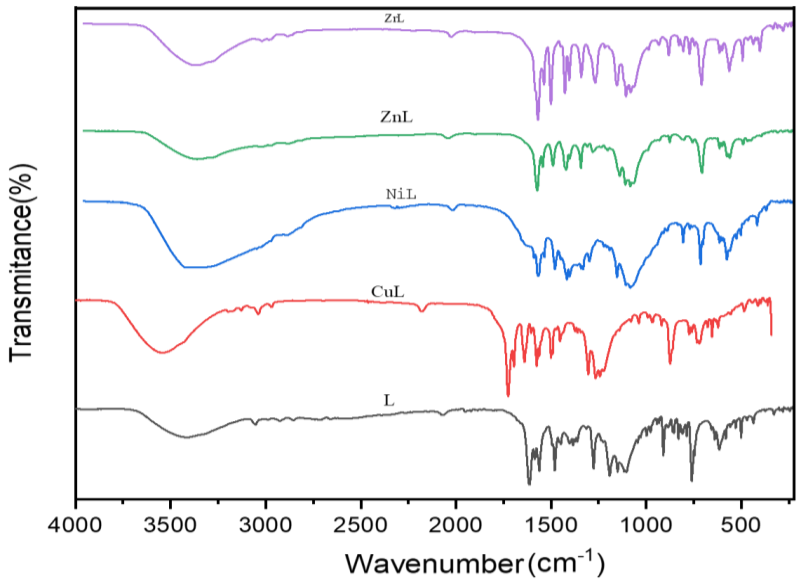

Fig. 3: FT-IR spectra of the ligand and its metal complexes

Table 2: FTIR spectral data of the ligand and metal complexes

Ligand/Metal complexes	FTIR/cm^{-1}				
	ν(O-H)	ν(C=N)	ν(C-O)	ν(M-O)	ν(M-N)
$C_{20}H_{16}O_2N_2(L^1)$	3466	1614	1193	-	-
$[ZnC_{20}H_{14}O_2N_2]$	3435	1607	1180	533	448
$[CuC_{20}H_{14}O_2N_2]$	3430	1609	1188	537	369
$[NiC_{20}H_{14}O_2N_2]$	3459	1610	1196	545	459
$[ZrC_{20}H_{14}O_2N_2](NO_3)_2$	3434	1609	1181	538	466

Electronic spectra and magnetic moment measurement

In DMSO at ambient temperature, the electronic spectra of the Schiff base and all metal complexes were taken (fig. 4). The magnetic moment values of the Schiff base ligand and its transition metal complexes, as well as their electronic absorption spectral data, are provided in table 3. The electronic spectra of the ligand have two absorption bands corresponding to n-π* and π-π* transitions. These transitions are present in the complexes' spectra as well, but they are shifted towards lower and higher frequencies, indicating that the ligand has coordinated with the metallic ions [13]. High-intensity absorption peaks at 277 nm and 339 nm in the electronic spectra of the ligand $[C_{20}H_{16}O_2N_2]$ have been attributed to the

π→π* and n→π* transitions, respectively [21]. The Zn(II) complex's UV-Vis spectra reveal the presence of three potent absorption bands at 265, 296, and 321 nm [22] The peak at 265 nm and 296 nm was assigned to π→π* and the peak at 321 nm is attributed to n→π* transition due to a lone pair of electrons of azomethine nitrogen and an antibonding orbital [23, 24]. Another absorption band at 395 nm in the spectra of the Zn(II) complex is probably because of ligand-to-metal charge transfer (LMCT) [21-24]. Electronic spectral data coupled with the magnetic moment value of the Zn(II) complex suggested the tetrahedral geometry of the [22]. The electronic absorption spectrum of the Cu(II) complex in DMSO solution showed three bands at 265 nm,320 nm, and 420 nm for π→π*, n→π*, and ligand-to-metal charge transfer (LMCT) respectively [25]. These data and the magnetic moment value of 0.60 B. M suggested tetrahedral geometry around Cu(II) [19]. The electronic absorption spectrum of the Ni(II) complex in DMSO solution showed four bands at 260 nm, 320 nm, 420 nm, and 480 nm for π→π*, n→π* ligand-to-metal charge transfer (LMCT) and $3A_{2g}$ (F)→$3T_{1g}$ (F) respectively [26, 27]. These data and the magnetic moment value of 0.48 B. M suggested square geometry around Ni(II) [26]. Similarly, the ZrO(IV) complex electronic data was investigated and its magnetic moment value was 1.40 μ B. M, suggesting the square pyramidal geometry [28].

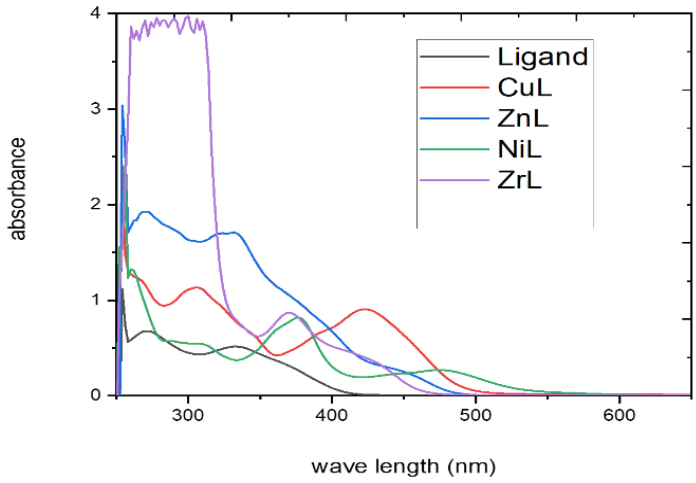

Fig. 4: Electronic spectra of the ligand and its metal complexes

Table 3: Magnetic moments and electronic spectral data for ligand (L) and its metal complexes

Compound	λ_{max} nm	Wave number cm^{-1}	μ_{eff} B. M.	Assignment	Geometry
$[C_{20}H_{16}O_2N_2]$	277	36101	_	π→π*	
	339	25062		n→π*	
$[ZnC_{20}H_{14}O_2N_2]$	265	37735		π→π*	
	296	33783	1.06	π→π*	Tetrahedral
	321	31152		n→π*	
	399	24691		C. T (M→L)	
$[CuC_{20}H_{14}O_2N_2]$	265	37735		π→π*	
	320	31250	0.60	n→π*	Tetrahedral
	420	23809		C. T (M→L)	
$[NiC_{20}H_{14}O_2N_2]$	260	38461		π→π*	
	320	31250	0.48	n→π*	Square planar
	420	23809		C. T (M→L)	
	480	20833		$3A_{2g}$(F)→$3T_{1g}$(F)	
$[ZrC_{20}H_{14}O_2N_2]$ $(NO_3)_2$	265	37735	1.40	π→π*	
	297	33670		π→π*	Square planar
	338	29585		n→π*	
	402	24875		C. T (M→L)	

Thermogravimetric analysis

The thermal decomposition analysis of solid Zn(II),Cu(II),Ni(II), and Zr(IV) complexes was carried out under a nitrogen atmosphere and the heating rate was suitably controlled at 30 °C/min and the weight loss was measured from the ambient temperature up to 800 °C. The data from Thermogravimetric analysis (TGA) indicated that the decomposition of the complexes proceeds in three or four steps. There were some minor steps and asymmetry of Thermogravimetric analysis (TGA) curves was also observed. The weight losses for each complex were calculated within the corresponding temperature ranges. The different thermodynamic parameters are listed in table 4.

$[ZnC_{20}H_{14}O_2N_2]$ complex

The Zn(II) complex's TGA curve (fig. 5a) showed that the complex was decomposed into three primary processes. The fraction of the ligand (-C_6H_4) was degraded in the first phase of decomposition in the temperature range 180-290 °C (calculated at 20.00% and experimental at 20.00%). In the second step at 290–600 °C, the remaining portion of the ligand ($C_{14}H_{10}O_2N_2$) was broken down (calculated 62.33%, experimental 60.10%)[27]. The combination disintegrated and was eliminated as Zn/ZnO (calculated 21.09%, experimental 20.00%) polluted with few carbon atoms at temperatures above 650 °C.

$$[ZnC_{20}H_{14}O_2N_2] \xrightarrow[-C_6H_4\ (Cal\text{-}20\%;Exp\text{-}20\%)]{180\text{-}290^{\circ}C} [ZnC_{14}H_{14}O_2N_2] \xrightarrow[-C_{14}H_{10}O_2N_2\ (Cal\text{-}62\%;Exp\text{-}60\%)]{550\text{-}650^{\circ}C} Zn/ZnO\ (Cal\text{-}21\%\text{-}Exp\text{-}20\%)$$

$[CuC_{20}H_{14}O_2N_2]$ complex

The thermogravimetric analysis (TGA) curve in (fig. 5b) suggested that the Cu(II) complex is thermally stable because it didn't degrade up to 200 °C[27]. In the first step, the part of ligand ($-C_6H_4$) (calculated 20.00%, experimental 20.00%) was decomposed at temperature 200-550 °C. In 2nd step, the decomposition of ($C_{14}H_{10}O_2N_2$) (calculated 62.0%, experimental 60.00 %)moiety was taken place at temperature 550-710 °C [25]. Finally, the complex was completely decomposed and removed as Cu/CuO (calculated 20.00%, experimental 20.00%) at above 710 °C [30].

$$[CuC_{20}H_{14}O_2N_2] \xrightarrow[-C_6H_4(Cal\text{-}20\%;Exp\text{-}20\%)]{200\text{-}550^{o}C} [CuC_{14}H_{10}O_2N_2] \xrightarrow[-C_{14}H_{10}O_2N_2(Cal\text{-}62\%;Exp\text{-}60\%)]{550\text{-}710^{o}C} Cu/CuO\ (Cal\text{-}20\%;Exp\text{-}20\%)$$

$[NiC_{20}H_{14}O_2N_2]$ complex

Indicating the absence of any lattice water molecules[1]. This complex was decomposed into three main steps, shown in fig. 5c. In the first step, the part of ligand ($-C_6H_4$) (calculated 18.00%, experimental 20.00%) was decomposed at temperature 300-400 °C. In 2ndstep, the decomposition of ($C_{14}H_{10}O_2N_2$-) (calculated 58.00%, experimental 60.00%) moiety took place at a temperature of 400-590 °C. Finally, the complex was completely decomposed and removed as Ni/NiO (calculated 18.0%, experimental 20%) [1, 2, 4].

The fragment scheme for the complex is shown below:

$$[NiC_{20}H_{14}O_2N_2] \xrightarrow[-C_6H_4(Cal\text{-}18\%;Exp\text{-}20\%)]{300\text{-}400^{o}C} [NiC_{14}H_{10}O_2N_2] \xrightarrow[-C_{14}H_{10}O_2N_2(Cal\text{-}58\%;Exp\text{-}60\%)]{400\text{-}590^{o}C} Ni/NiO\ (Cal\text{-}18\%;Exp\text{-}20\%)$$

$[ZrC_{20}H_{14}O_2N_2]$ complex

The Zr(IV) complex showed high thermal stability and decomposed above 250 °C, indicating the absence of any lattice water molecules[1]. This complex was decomposed into three main steps shown in fig. 5d. In the first step, the part of ligand ($-C_6H_4$) (calculated 21.00%, experimental 15.00%) was decomposed at temperature 300-450 °C. In 2ndstep, the decomposition of ($-C_{14}H_{10}O_2N_2$) (calculated 56.0%, experimental 57.00%) moiety took place at temperature 450-770 °C. Finally, the complex was completely decomposed and removed as ZrO/ZrO_2 (calculated 27.00%, experimental 28.00%) [30].

The fragment scheme for the complex is shown below:

$$[ZrC_{20}H_{14}O_2N_2] \xrightarrow[-C_6H_4\ (Cal\text{-}21\%;Exp\text{-}15\%)]{300\text{-}450^{\circ}C} [ZrC_{14}H_{14}O_2N_2] \xrightarrow[-C_{14}H_{10}O_2N_2\ (Cal\text{-}56\%;Exp\text{-}57\%)]{450\text{-}770^{\circ}C} Zr/ZrO\ (Cal\text{-}27\%\text{-}Exp\text{-}28\%)$$

Table 4: Thermal data of Zn(II), Cu(II), Ni(II) and Zr(IV) complexes of ligand $C_{20}H_{16}O_2N_2$ (L)

Complexes	Steps	Temperature range/°C	TG mass loss % calc./found	Assignments
$[ZnC_{20}H_{14}O_2N_2]$	1st	180-290	20.00/20.00	C_6H_4
	2nd	550-650	62.33/60.10	$C_{14}H_{10}O_2N_2$
	3rd	>600	21.09/20.00	Zn/ZnO
$[CuC_{20}H_{14}O_2N_2]$	1st	400-450	20.00/20.00	C_6H_4
	2nd	450-600	62.00/60.00	$C_{14}H_{10}O_2N_2$
	3rd	>600	20.00/20.00	Cu/CuO
$[NiC_{20}H_{14}O_2N_2]$	1st	400-500	18.00/20.00	C_6H_4
	2nd	500-650	58.00/60.10	$C_{14}H_{10}O_2N_2$
	3rd	>650	18.00/20.00	Ni/NiO
$[ZrC_{20}H_{14}O_2N_2]\ (NO_3)_2$	1st	300-450	21.00/15.00	C_6H_4
	2nd	450-770	56.00/57.00	$C_{14}H_{10}O_2N_2$
	3rd	>770	27.00/28.00	Zr/ZrO

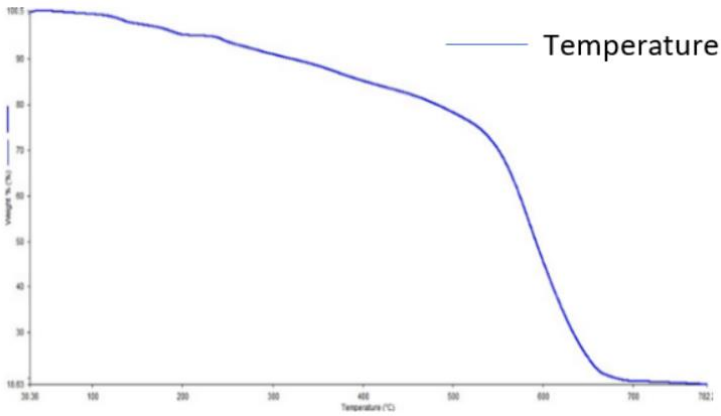

Fig. 5a: TGA curve of $[ZnC_{20}H_{14}O_2N_2]$

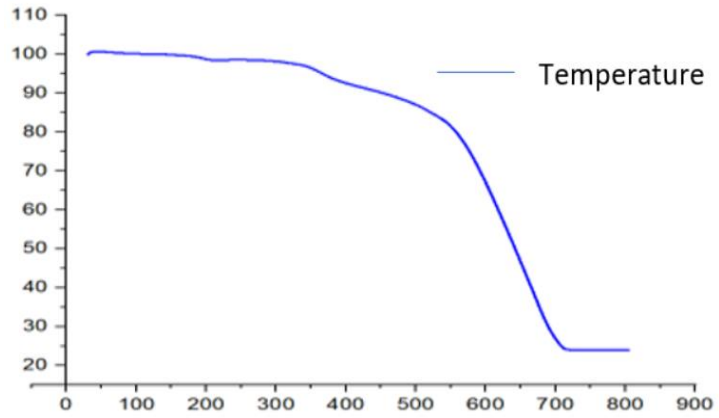

Fig. 5b: TGA curve of [$CuC_{20}H_{14}O_2N_2$]

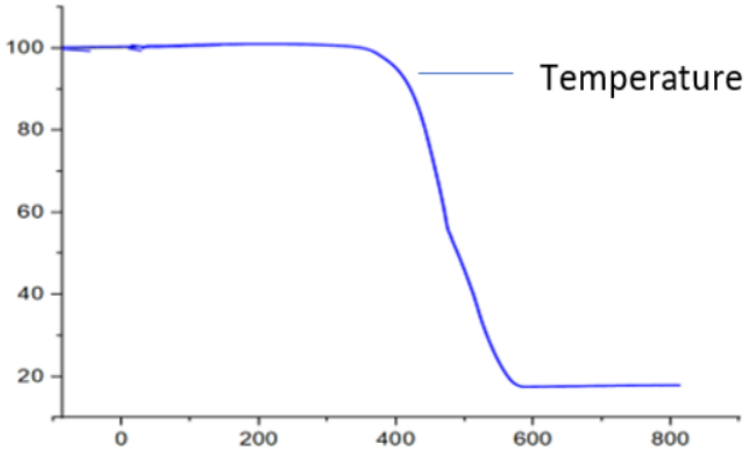

Fig. 5c: TGA curve of [$NiC_{20}H_{14}O_2N_2$] complex

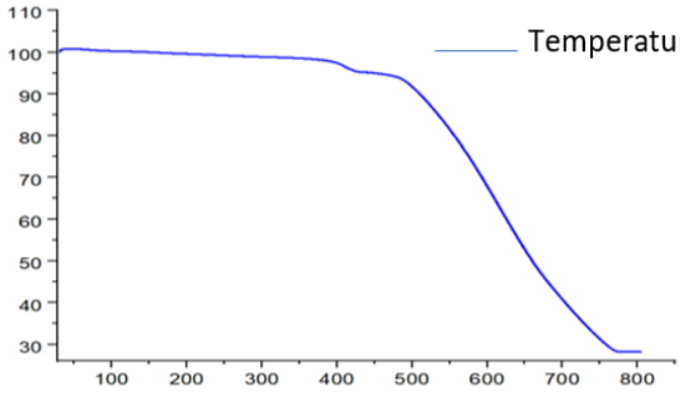

Fig. 5d: TGA curve of [$ZrC_{20}H_{14}O_2N_2$] $(NO_3)_2$ complex

Antibacterial activity

The prime objective of performing the antibacterial screening is to determine the susceptibility of the pathogenic microorganism. The free Schiff base ligand and their metal complexes were screened for their antibacterial activity against [39], *Bacillus cereus*-, *Escherichia coli*-, *Shigella boydii* and *Staphylococcus aureus*. The bacterial strains were obtained from Molecular Health Science Laboratory, Department of Genetic Engineering and Biotechnology, University of Rajshahi. The compounds were tested at a concentration of 50 µg/0.01 ml in DMSO solution using the paper disc diffusion method. The susceptibility zones were measured in diameter (mm) and the results were listed in table 5. The susceptibility zones were the clear zones around the discs killing the bacteria. All the Schiff base and metal complexes individually exhibited varying degrees of inhibitory effects on the growth of tested bacterial species (fig. 6).

Table 5: Antibacterial screening (zone of inhibition in mm) of schiff base ligand and its metal complexes

Compound	*E. coli*	*S. boydii*	*S. aureas*	*B. cereus*
DMSO	6.00±00	6.00±00	6.00±00	6.00±00
L	9.33±0.58	11.83±0.29	9.40±0.40	9.27±0.31
NiL	6.67±0.58	6.00±00	6.00±00	6.00±00
ZrL	7.67±0.58	7.17±0.29	9.23±0.25	7.17±0.29
CuL	14.83±0.76	10.43±0.40	8.17±0.29	9.13±0.32
ZnL	8.83±0.76	11.47±0.50	11.93±0.40	13.83±0.76
Kanamycine	26.67±1.53	23.00±1.00	19.67±0.58	25.33±0.58

Results provided as mean±SD (This experiment done three times, n=3)

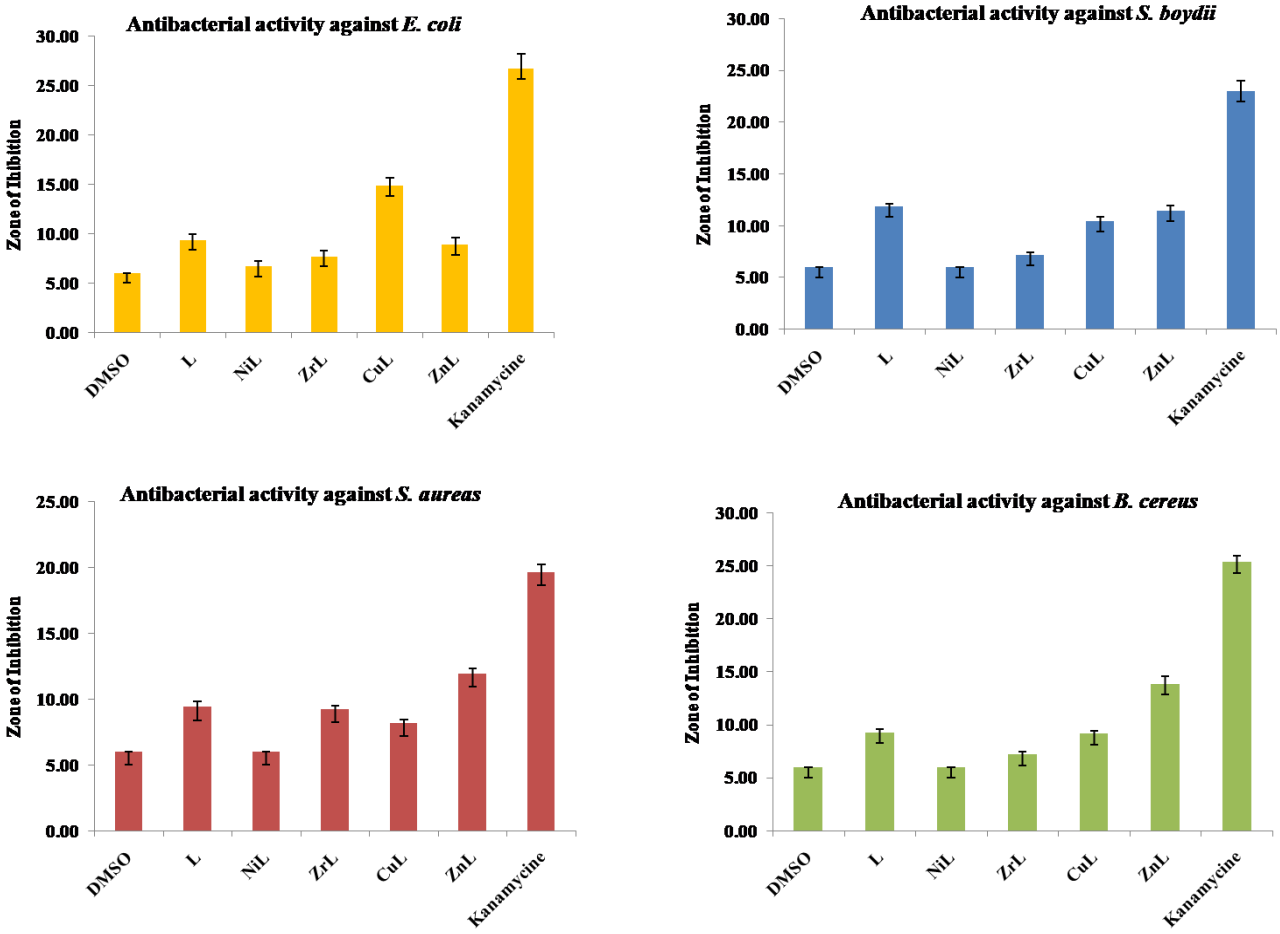

Fig. 6: Antibacterial screening activity of schiff base ligand and its metal complexes (mean±SD, n=3)

Brine shrimp cytotoxicity test

The synthesized product was tested for its cytotoxicity against Artemia salina (brine-shrimps eggs) using the standard protocol [31].

Experimental design for cytotoxicity test

The eggs of brine shrimps are hatched in simulated saltwater to get nauplii. This is done to obtain nauplii. The fabrication of test samples requires the addition of a determined amount of DMSO (dimethyl sulfoxide) to produce the requisite concentration of the test sample. This happens to ensure that the test sample is accurate. After the nauplii have been counted via a visual inspection, they are then moved into a test tube that has five milliliters of water and placed inside of it. A micropipette is next used to transfer the samples of varied concentrations into the test tube that has been specified in advance. This step comes after the previous one. A comparative analysis was performed between the cytotoxicity of the test agents and the cytotoxicity of the negative control that was produced.

Preparation of simulated seawater (brine water)

Since the lethality test requires the cultivation of brine shrimp nauplii, the nauplii must be cultured in seawater. The amount of sodium chloride found in seawater is 3.8%. Therefore, a solution of sodium chloride with a concentration of 3.8% was produced by dissolving 38 gs of sodium chloride (NaCl) in one liter of distilled water and then filtering the solution. Using NaHCO3, the pH of the brine water that was created in this manner was kept between 8 and 9 throughout the process.

Hatching of brine shrimps

The brine shrimp's cysts were collected from classic aquarium shops in Rajshahi, Bangladesh. A solution of 38 g of sea salt and one liter of distilled water was used to create artificial saltwater, which was then used to hatch brine shrimp eggs, which belong to the species Artemia salina Leach. Following an incubation period of forty-eight hours at room temperature (27-29 °C) [32-34], the larvae (nauplii) were harvested using a pipette after being drawn to one side of the jar while a light source was present. After being aliquoted three times in tiny beakers containing saltwater, the nauplii were extracted from the eggs and separated from the eggs [35].

Samples preparation and application

In this work, the production of synthetic compounds at different concentrations, ranging from 50 to 400 µg/ml, was the subject of investigation. Sample solutions with concentrations of 50, 100, 200, and 400 µg/ml were transferred to separate vials that were clean to facilitate the process of evaporating the solvent. After that, a flow hood was placed over these sample vials. Each vial contained thirty shrimp and one milliliter of simulated saltwater. The shrimp were put into the vials. Using simulated saltwater, the volume of the completed product was raised to five milliliters, and the pH was adjusted to 7.4 to get the desired result. Vials that were used as the negative control (solvent system) were subjected to an approach that was quite like the one described before. Each vial was exposed to incubation at a temperature of 26 ±1 °C for twenty-four hours, during which time it was further lit. The number of shrimp that had survived was then counted in both the control and test vials and the median lethal concentrations (LC50) were calculated by employing the dose-response curve in combination with the Microsoft Excel program [35]. This was done after the previous step had been completed.

The actual mortility % was calculated with the following formula:

$$(TN\text{-}AN)/TN \times 100$$

Here,

TN= Taken Nauplii

AN=Alive Nauplii

Table 6: Cytotoxicitytestof schiff base ligand and its metal complexes

Sample	Concentration of sample/µg/ml	Log C	% mortality	LC_{50} µg/ml
Standard (vincristine sulphate)	31.25	1.49494	41.67±2.89	35.17±3.39
	62.5	1.79239	51.67±2.89	
	125	2.09691	70.00±5.00	
	250	2.39794	75.00±5.00	
	500	2.69897	83.33±2.89	
L	31.25	1.49494	18.33±2.89	308.29±3.65
	62.5	1.79239	35.00±5.00	
	125	2.09691	40.00±8.66	
	250	2.39794	51.67±2.89	
	500	2.69897	66.67±2.89	
[Cu(L)]	31.25	1.49494	26.67±2.89	250.87±6.72
	62.5	1.79239	45.00±5.00	
	125	2.09691	58.33±7.64	
	250	2.39794	68.33±2.89	
	500	2.69897	76.67±2.89	
[Ni(L)]	31.25	1.49494	11.67±2.89	301.59±12.37
	62.5	1.79239	18.33±2.89	
	125	2.09691	33.33±5.77	
	250	2.39794	55.00±5.0	
	500	2.69897	71.67±2.89	
[Zn(L)]	31.25	1.49494	18.33±2.89	268.09±7.32
	62.5	1.79239	28.33±5.77	
	125	2.09691	35.00±5.00	
	250	2.39794	58.33±2.89	
	500	2.69897	81.67±2.89	
[Zr(L)]	31.25	1.49494	18.33±2.89	268.09±7.59
	62.5	1.79239	31.67±7.64	
	125	2.09691	50.00±5.00	
	250	2.39794	56.67±2.89	
	500	2.69897	78.33±2.89	

Results provided as mean±SD (This experiment done three times, n=3)

Antioxidant test

The assessment of the antioxidant characteristics of l and its metal ion complexes was conducted utilizing DPPH, a free radical molecule. The DPPH radical scavenging activity of metal complexes L, and BHT (butylated hydroxytoluene) is presented as a percentage in table 2. The results indicated that all the metal complexes exhibited a moderate level of DPPH radical scavenging activity (fig. X). It is possible to express the sequence as follows: BHT>CuL>NiL>ZnL>L. An analogous pattern was noted regarding the metal complexes that were produced from the l ligand. Cu^{2+}complexes exhibit greater antioxidant activity in both instances compared to other complexes synthesized. The metal complexes derived from the ligand (L) exhibit significantly higher DPPH scavenging activity than the free ligand (L). This indicates that the complexes function as effective antioxidants and free radical scavengers compared to the free ligand (L), albeit at a lower level than standard BHT. It was demonstrated that the radical-scavenging

activity of both the standard BHT and the metal complexes increased with increasing concentration. A significant improvement in the antioxidant properties of the ligands was observed upon chelation with transition metal ions. The oxidizing potentials (OP) of the complexes are determined by the presence of compounds whose actions involve the contribution of hydrogen atoms to disrupt the chain of free radicals [37,38]. Thus, the results of this investigation suggest that CuL and ZnL complexes have the potential to be utilized in the treatment of pathological conditions caused by oxidative stress. The IC_{50} values of each compound mentioned in conjunction with the standard BHT have been computed and are presented in tables 7.

Table 7: % of scavenging activity of Schiff base ligand and its metal complexes

Conc (µg/ml)	BHT	L	CuL	NiL	ZnL	ZrL
20	9.24±0.25	1.5±0.15	4.74±0.54	1.87±0.32	3.53±0.53	4.62±0.83
40	15.82±2.24	2.33±0.39	8.65±0.48	3.9±0.54	5.86±0.32	7.69±0.27
60	28.08±0.33	2.54±0.16	12.06±0.96	5.93±0.69	7.13±0.72	9.21±0.53
80	34.08±2.77	3.3±0.23	13.41±0.74	8.77±0.42	9.58±0.40	11.05±0.58
100	38.97±1.59	3.77±0.15	16.43±0.91	12.98±0.82	10.94±0.68	14.22±0.37
IC_{50}	6.19±0.25	89±3.18	16.87±0.57	19.66±0.61	26.01±0.91	20.5±2.38

Results provided as mean±SD(This experiment done three times, n=3)

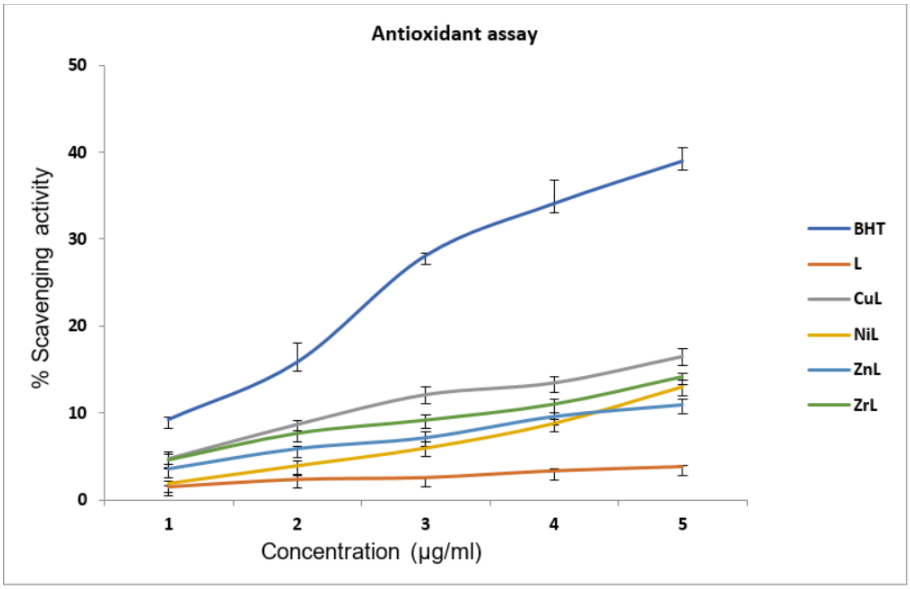

Fig. 6: DPPH radical scavenging activity of Schiff base ligand and its metal complexes with standard BHT mean±SD, n=3

CONCLUSION

Cu(II), Zn(II), Ni(II), and Zr(IV) ions with a Schiff base ligand were synthesized and studied. The ligand was produced by condensing salicylaldehyde with o-phenylenediamine. Electronic spectra and magnetic susceptibility data revealed tetrahedral geometry for $[ZnC_{20}H_{14}O_2N_2]$ and $[CuC_{20}H_{14}O_2N_2]$, and square planar geometry for $[NiC_{20}H_{14}O_2N_2]$ and $[ZrC_{20}H_{14}O_2N_2]$. Thermal analysis showed the complexes were mostly thermally stable with a possible degradation pathway. Biological activity tests indicated that the ligand and its metal complexes exhibited moderate to strong antibacterial activity, with the metal complexes being more effective than the Schiff base ligand alone.

ACKNOWLEDGMENT

The authors are thankful to the Chairman, Department of Chemistry, University of Rajshahi Rajshahi-6205, Bangladesh, for the laboratory facilities.

FUNDING

Faculty of Science, University of Rajshahi Rajshahi-6205, Bangladesh.

AUTHORS CONTRIBUTIONS

The authors contributed equally to the experimental design, analysis, and interpretation. Each author participated in drafting and revising the manuscript critically for important intellectual content, approving the final version for publication.

CONFLICT OF INTERESTS

The authors declare no conflicts of interest regarding the publication of this experimental article.

REFERENCES

1. Dinnimath BM, Gowda P, Naik A. Development of organometallic compounds of Schiff bases with diverse applications. Int J Pharm Pharm Sci. 2023;15(6):1-15. doi: 10.22159/ijpps.2023v15i6.47362.

2. Xavier DA, Srividhya N. Synthesis and study of Schiff base ligands. IOSRJAC. 2014;7(11):6-15. doi: 10.9790/5736-071110615.
3. Worku D, Negussie M, Raju VJ, Theodros S, Jonson JA. Studies of transition metal complexes of herbicidal compounds II transition metal complexes derivatized from 2-chloro-4-ethylamino-6-isopropylamino-S-triazine(atrazine). Chem Soc Ethiopia. 2003;17(1):35-43. doi: 10.4314/bcse.v17i1.61728.
4. Arun V, Sridevi N, Robinson PP, Manju S, Yusuff KK. Ni(II) and Ru(II) Schiff base complexes as catalysts for the reduction of benzene. Journal of Molecular Catalysis a: Chemical. 2009;304(1-2):191-8. doi: 10.1016/j.molcata.2009.02.011.
5. Sudhasankar S. Synthesis biological study DNA interaction of mannich base metal complexes derived from benzamide. Int J Curr Pharm Sci. 2021;13(6):60-4. doi: 10.22159/ijcpr.2021v13i6.1917.
6. Shrivastava S, Ahuja D. Synthesis and antimicrobial screening of 2,6-diamino pyridine schiff bases of isatin derivatives. Int J Curr Pharm Sci. 2022 Dec 14;15(1)47-50. doi: 10.22159/ijcpr.2023v15i1.2071.
7. DE Souza AO, Galetti FC, Silva CL, Bicalho B. Pharma MM, Fonseca SF. Antimycobacterial and cytotoxicity activity and natural compounds. Quim Nova. 2007;30(7):1563-6. doi: 10.1590/S0100-40422007000700012.
8. Przybylski P, Huczynski A, Pyta K, Brzezinski B, Bartl F. Biological properties of schiff bases and azo derivatives of phenols. Curr Org Chem. 2009;13(2):124-48. doi: 10.2174/138527209787193774.
9. Pahontu E, Julea F, Rosu T, Purcarea V, Chumakov Y, Petrenco P. Antibacterial antifungal and *in vitro* antileukaemia activity of metal complexes with thiosemicarbazones. J Cell Mol Med. 2015;19(4):865-78. doi: 10.1111/jcmm.12508, PMID 25708540.
10. Shariar SM, Jesmin M, Ali MM. Antibacterial activities of some schiff bases involving thiosemicarbazide and ketones. ILCPA. 2014 Jan;26:53-61. doi: 10.56431/p-40j3lb.
11. Kumar G, Kumar D, Singh CP, Kumar A, Rana VB. Synthesis physical characterization and antimicrobial activity of trivalent metal shiff base complexes. J Serb Chem Soc. 2010;75(5):629-37. doi: 10.2298/JSC090704037K.
12. Dalia M, Afsan F, Hossain M, Mannan M, Haque M, Kudrat E Zahan M. Spectral and thermal characterization of Mn(II) Ni(II) and Zn(II) complexes containing schiff base ligands towards potential biological application. AJOCS. 2018;4(4):1-11. doi: 10.9734/AJOCS/2018/42355.
13. Afsan F, Dalia SA, Hossain S, Sarker S, E Zahan KE. Synthesis spectral and thermal characterization of selected metal complexes containing schiff base ligands with antimicrobial activities. AJOCS. 2018;4(3):1-19. doi: 10.9734/AJOCS/2018/40913.
14. Shampa JA, Islam MR, Hossain MS, Rahman GT, Zakaria CM, Zahan KE. Physiochemical and antibacterial activity investigation on noble schiff base Cu (II) complex. Am J Heterocycl Chem. 2017;3(4):37-41.
15. Hossain MS, Zakaria CM, Zahan MK. Synthesis and characterization with antimicrobial activity studies on some transition metal complexes of N,O donor novel schiff base ligand. J Sci Res. 2017;9(2):209-18. doi: 10.3329/jsr.v9i2.29780.
16. Hossain MS, Sarker S, Shaheed AS, Hossain MM, Alim Al Bari A, Karim MR. Thermal and spectral characterization of Cr(III) Co(II) and Cd(II) metal complexes containing bis-imine novel schiff base ligand towards potential biological application. Chem Biomol Eng. 2017;2(1):41-50. doi: 10.11648/j.cbe.20170201.16.
17. Dubourdieu DJ, Nalla S, Talukdar J, Shier WT. Characterization studies on a tetrahydro curcumin zinc complex. Int J Pharm Pharm Sci. 2022;14(10):24-7. doi: 10.22159/ijpps.2022v14i11.44720.
18. Eco-friendly and efficient composition diagnosis theoretical kinetic studies antibacterial and anticancer activities of mixed some metal complexes of tridentate schiff base ligand. IJPR. 2021;13(1). doi: 10.31838/ijpr/2021.13.01.428.
19. Hemalatha GM, Thirunavukkarasu K, Kumar CR. Isoniazid-based schiffs bases in bone cancer studies using MG-63 cell lines. Int J App Pharm. 2022;14:168-74. doi: 10.22159/ijap.2022.v14ti.48.
20. Narasimhavarman S, Rajasekar K, Mandal SK, Selvarani R, Veeravel C. *In vitro* anticancer antioxidant and molecular docking studies of 4-aminobenzamide metal complexes. Int J App Pharm. 2022;14:175-9. doi: 10.22159/ijap.2022.v14ti.51.
21. Al Shemary RK, Numan AT, Atiyah EM. Synthesis characterization and antimicrobial evaluation of mixed ligand complexes of manganese(II) cobalt (II) copper(II) nickel(II) and mercury(II) with 1,10 phenanthroline and a bidentateschiff base. Eur Chem Bull. 2016;5(8):335-8.
22. Elachi KA, Hossain MS, Bitu MN, Zahid AA, Mohapatra RK, Mannan MA. synthesis spectral and thermal characterization on bioactive complexes of Mg(II) Zn(II) ions containing schiff base ligand. J Chem Bio Phy Sci Section A(II) Vo(II) and Bi. 2019;9(4):201-18.
23. Gondia NK, Priya J, Sharma SK. Synthesis and physic-chemical characterization of a schiff base and its zinc complex. Res Chem Intermed. 2017;43(2):1165-78. doi: 10.1007/s11164-016-2690-9.
24. Hossain MS, Shaheed AS, Khan MN, Mannan MA, Haque MM, Zakaria CM. Synthesis and characterization of Cu(II) and Co (II) complexes containing schiff base ligands towards potential biological application. J Chem Bio Phy Sci. 2018;8(4):654-68 . doi: 10.24214/jcbps.A.8.4.65468.
25. Camellia FK, Ashrafuzzaman M, Islam MN, Banu LA, Kudrat E Zahan MK. Synthesis characterization and thermal study of some transition metal complexes of N-(4-hydroxybenzylidene)isonicotinohydrazone and investigation of their antibacterial and antioxidant properties. AJOCS. 2022;11(4):8-22. doi: 10.9734/ajocs/2022/v11i419130.
26. Raman N, Ravichandran S, Thangaraja C. Copper(II) cobalt(II) nickel(II) and zinc(II) complexes of schiff base derived from benzil-2,4-dinitrophenylhydrazone with aniline. J Chem Sci. 2004;116(4):215-9. doi: 10.1007/BF02708270.
27. Shiraj U Ddula M, Islam MA, Akhter S, Islam MK, Zahan MK. Synthesis characterization and antimicrobial activity of Cd(II) Ni(II) Co(II) and Zr(IV) metal complexes of schiff base ligand derived from diethylenetriamine and isatin. Asian J Res Chem. 2014;7(7):45-9.
28. Sumar Ristovic MT, Minic DM, Poleti D, Miodragovic Z, Miodragovic D, Andelkovic KK. Thermal stability and degradation of Co(II) Cd(II) and Zn(II) complexes with N-benzyloxycarbonylglycinato ligand. J Therm Anal Calorim. 2010;102(1):83-90. doi: 10.1007/s10973-010-0748-2.
29. Hossain MS, Zakaria CM, Zahan MK, Zaman B. Synthesis spectral and thermal characterization of Cu(II) complexes with two new schiff base ligand towards potential biological application. Der Pharma Chemica. 2017;8(3):380-92.
30. Meyer B, Ferrigni N, Putnam J, Jacobsen L, Nichols D, Mc Laughlin J. Brine shrimp: a convenient general bioassay for active plant constituents. Planta Med. 1982;45(5):31-4. doi: 10.1055/s-2007-971236.
31. Habala L, Varenyi S, Bilkova A, Herich P, Valentova J, Kozisek J. Antimicrobial activity and urease inhibition of schiff bases derived from isoniazid and fluorinated benzaldehydes and of their copper(ii) complexes. Molecules. 2016;21(12):1742. doi: 10.3390/molecules21121742, PMID 27999327.
32. Ramachandran S, Shanmugapandiyan P, Nalini CN. Synthesis and anti-microbial evaluation of N-(2-(4-substituted phenyl)-4-oxothiazolidin-3-yl) isonicotinamide derivatives. Int J Pharm Sci Res. 2011;2(6):1564-8. doi: 10.13040/IJPSR.0975-8232.2(6).1564-68.
33. Abou Melha KS. Transition metal complexes of isonicotinic acid (2-hydroxybenzylidene)hydrazide. Spectrochim Acta A Mol Biomol Spectrosc. 2008;70(1):162-70. doi: 10.1016/j.saa.2007.07.023, PMID 17728178.
34. Ahmed MN, Yasin KA, Ayub K, Mahmood T, Tahir MN, Khan BA. Click one pot synthesis spectral analyses crystal structures DFT studies and brine shrimp cytotoxicity assay of two newly synthesized 1,4,5-trisubstituted 1,2,3-triazoles. J Mol Struct. 2016;1106:430-9. doi: 10.1016/j.molstruc.2015.11.010.
35. Joseph J, Nagashri K, Rani GA. Synthesis characterization and antimicrobial activities of copper complexes derived from 4-aminoantipyrine derivatives. J Saudi Chem Soc. 2013;17(3):285-94. doi: 10.1016/j.jscs.2011.04.007.
36. Camellia FK, Ashrafuzzaman M, Islam MN, Banu LA, Kudrat E Zahan MK. Synthesis characterization antibacterial and antioxidant studies of isoniazid-based schiff base ligands and their metal complexes. AJACR. 2022:11(3):8-23. doi: 10.9734/ajacr/2022/v11i330257.

37. Saadh MJ, Al Wahish MA. Evaluation of the potential cytotoxicity of ruthenium complex II against U-373 glioblastoma cells. Int J App Pharm. 2023;15(6):218-21. doi: 10.22159/ijap.2023v15i6.48940.
38. Baskaran K, Nirmaladevi N, Ilangovan M. Antioxidant properties *Cladophora socialis* green algae of seaweeds collected from Rameswaram in India. Int J Curr Pharm Res. 2022;14(6):24-31. doi: 10.22159/ijcpr.2022v14i6.2042.
39. Shrivastava S, Ahuja D. Synthesis and antimicrobial screening of 2,6-diaminopyridine schiff bases of isatin derivatives. Int J Curr Pharm Sci. 2023;15(1):47-50. doi: 10.22159/ijcpr.2023v15i1.2071.